

# Specificities of boron disubstituted sumanenes

Stevan Armaković · Sanja J. Armaković ·  
Jovan P. Šetrajčić · Ljubiša D. Džambas

Received: 18 August 2012 / Accepted: 14 October 2012 / Published online: 13 November 2012  
© Springer-Verlag Berlin Heidelberg 2012

**Abstract** In this article we focused on computational research of sumanenes disubstituted by boron where the two carbon atoms are substituted by two boron atoms. Disubstitution of rim carbon atoms with boron atoms significantly affected the geometry of the bowl. The main stability factors were used to determine the stability of isomers. The most stable, the shallowest and the deepest isomers were subjected to further study of NMR parameters, chemical shielding and NICS, aromaticity, bowl to bowl inversion barrier and NBO/NPA analysis. The introduction of boron atoms significantly affected the above parameters, changing the aromatic nature of rings, reducing bowl to bowl inversion barrier and produced charge transfer. The NICS are correlated with bowl depth having the result that the function of the fourth degree of bowl depth does not only correlate well to the bowl to bowl inversion barrier with bowl depth, but also finely correlates the change of the NICS and NICS<sub>zz</sub> with bowl depth.

**Keywords** Boron disubstituted sumanenes · Bowl to bowl inversion barrier · NMR parameters · NBO/NPA analysis

## Introduction

Bowl-shaped polyaromatic hydrocarbons, or  $\pi$ -bowls, are considered to be important structures whose research can significantly increase the potential of important interdisciplinary fields such as catalysis, pharmacy and electrical material science [1, 2]. There are two main factors that correlate  $\pi$ -bowls, such as coranulene and sumanene with fullerenes and nanotubes. The first is that the aforementioned compounds serve as model compounds of fullerenes and nanotubes, and the second is that these structures serve as potential synthetic intermediates for the artificially-designed fullerene derivatives such as hetero-fullerenes [2].

The importance of investigation of  $\pi$ -bowls, as main constituents of fullerenes and nanotubes, lie in the fact that the later mentioned can be easily modified [3, 4] by encapsulation, covalent linking,  $\pi$ -stacking and similar. Of course, it is not necessary to comment on the importance of fullerenes and nanotubes in all interdisciplinary fields of science. There are numerous, both theoretical and experimental, concrete examples of research of functionalized and doped fullerenes and nanotubes which take advantage from the delocalized  $\pi$ -electron density along the backbone [5].

The fact is that fullerenes containing boron, bora-fullerenes, have already been commented on in detail in the work of Vostrowsky and Hirsch [6] opens the possibility for further investigations. Also well-known  $\pi$ -bowl structure, coranulene, has already been treated computationally in a similar way [7].

Typical representatives of  $\pi$ -bowls are coranulene ( $C_{20}H_{10}$ ,  $C_{5v}$  symmetry) and sumanene ( $C_{21}H_{12}$ ,  $C_{3v}$  symmetry), Fig. 1. Coranulene was synthesized in 1966, and

---

S. Armaković (✉) · J. P. Šetrajčić  
Department of Physics, Faculty of Sciences,  
University of Novi Sad,  
Trg Dositeja Obradovića 4,  
21000 Novi Sad, Vojvodina, Serbia  
e-mail: stevan.armacovic@df.uns.ac.rs

S. J. Armaković  
Department of Chemistry, Biochemistry and Environmental  
Protection, Faculty of Sciences, University of Novi Sad,  
Trg Dositeja Obradovića 3,  
21000 Novi Sad, Vojvodina, Serbia

L. D. Džambas  
Department of Dentistry, Medical Faculty, University of Novi Sad,  
Hajduk Veljkova 3,  
21000 Novi Sad, Serbia

J. P. Šetrajčić  
Academy of Sciences and Arts of Republic of Srpska,  
Bana Lazarevića 1,  
78000 Banja Luka, B&H, Republic of Srpska

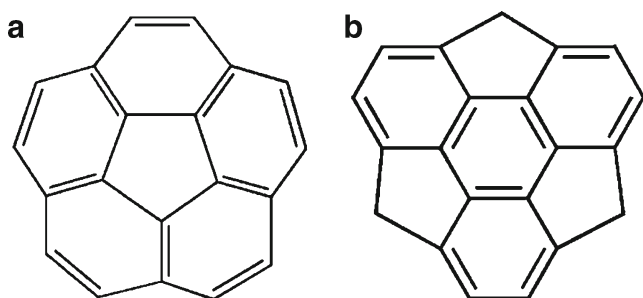


**Fig. 1** **a** Coranulene and **b** Sumanene

since then it has been studied intensively [7, 8] and many structures have been related to it. On the other side, research of sumanene practically started in 2003 [8] when it was synthesized by Hirao's group [2].

The three  $sp^3$  hybridized carbon atoms at the benzylic positions are the characteristic structural features of sumanene, which is in contrast to the coranulene, the rim of which is covered with five aromatic rings [1]. The advantages of sumanene concerning its three benzylic positions is that such structure may allow further functionalization of new bowl shaped structure [9].

Primary attempts for the synthesis of sumanene included planar aromatic compounds as initial one, but such synthesis failed due to the strain energy [1, 10]. This problem was overcome by construction of three-dimensional framework mostly based on tetrahedral  $sp^3$  carbons, which lead to the required  $\pi$ -conjugated structure by oxidative aromatization [1, 2].

The characteristic quantity for molecular bowls is the depth (bowl depth) of such structures, defined as a distance between the planes of hub benzene ring and aromatic carbon rim, Fig. 2. Sumanene is a deeper molecular bowl than coranulene, with depths of 1.11 Å and 0.89 Å respectively.

For the investigation of effects obtained by the substitution of carbon atoms with boron we mainly used NMR parameters, chemical shielding [11] that are very sensitive to the change of charge density and therefore are ideal parameters for comparison of similar or in some way perturbed systems. In addition, the calculations of (NMR) parameters using *ab initio* techniques have found the ability of quickly evaluating and correlating the magnitude of the chemical shielding (CS) tensors with variations in bond angles, bond lengths, and the nearest neighboring interactions and then have increased the significance of utilizing these parameters in investigations of molecular structures [12–14].



**Fig. 2** Bowl depth

For the evaluation of aromaticity Schleyer et al. [15] introduced nucleus independent chemical shifts (NICS) as a negative value of absolute magnetic shielding calculated at the aromatic ring center or one angstrom above the molecular plane. NICS are very important parameters because they are closely related to the energetic, structural and magnetic properties of molecules [16–18]. In this paper a correlation of NICS change with bowl depth has also been made.

Important quantity for molecular bowl is also a bowl to bowl inversion barrier which shows how prone the molecular bowl is to inversion. This quantity is determined for further investigated structures in this paper.

Natural bond order (NBO) analysis, performed in our work, is in general a fine approach to gain a good insight into the stability of molecules. Charges of atoms obtained with natural population analysis (NPA), for which is known to bring reliable data, have also been discussed in this paper.

### Computational details

Density functional theory calculations were performed by means of the hybrid, non-local exchange and correlation functional of Becke-Lee, Parr and Yang (B3LYP) [19, 20]. Two stages took place for all isomers: first the ground state geometrical parameters have been determined using 6-31G(d) atomic basis set. Secondly, harmonic vibrational spectrum of each isomer has been checked in order to assure that the true minimum of potential energy, to which corresponds only positive frequencies, is located. We decided to employ 6-31G(d) basis set for two main reasons. It has been shown that this basis set accurately reproduces the results obtained for the bowl-to-bowl inversion barrier of corannulene [8]. Secondly, this basis set is used in a significant number of papers dealing with theoretical research of carbon nanotubes and it is our goal in the near future to compare various properties of sumanene and carbon nanotubes, since buckybowl serve as model compounds of fullerenes and nanotubes [2].

The main idea was to check stability of investigated structures and to subject them to further investigation by calculation of chemical shielding, NICS and bowl to bowl inversion barrier. In this paper isomers which, according to parameters of HOMO-LUMO gap and chemical hardness, are the most stable as well as the shallowest and the deepest are further investigated. In this way we can investigate the effect of disubstitution on the stability, NMR parameters and bowl to bowl inversion barrier.

GIAO method [21] on the same level of theory was employed to calculate the NMR parameters; chemical shielding and NICS that we brought in correlation with bowl depth. The NICS values were obtained as negative of the

isotropic shielding calculated at the center of rings in each molecule [15–18].

In this paper we also decided to correlate the value of NICS along the direction connecting the centers of hub and rim of molecular bowl in order to investigate the influence of bowl-depth on the NICS values.

For all calculations we used Gaussian 03 [22].

## Results and discussion

### Stability

By optimizing the structures we obtained data on the HOMO and LUMO energies that we continue to utilize to calculate the parameters that indicate the stability/reactivity, such as the chemical potential  $\chi_m$  and chemical hardness  $\eta$ . Within the Koopmans' theorem these parameters can be calculated as follows:

$$\eta = +0.5(E_{LUMO} - E_{HOMO}) \quad (1)$$

$$\chi_m = -0.5(E_{HOMO} + E_{LUMO}) \quad (2)$$

These parameters are important as a measure of stability and sensitivity of organic compounds.

HOMO and LUMO are the main orbitals that take part in chemical stability [23]. The decrease in the HOMO and LUMO energy gap explains the intramolecular charge transfer interaction taking place within the molecule which is responsible for the activity of the molecule. A molecule with a small or no HOMO-LUMO gap is chemically reactive. Pearson showed that the HOMO-LUMO gap represents the

chemical hardness of the molecule [23], which has been used as an electronic property to characterize the relative stability of molecules. According to the principle of maximum hardness [24], the hardness of a system becomes maximal at equilibrium geometries [25], and the stability is directly related to the higher values of hardness [26].

Further, we summarize results concerning stability factors and bowl depth in Fig. 3, while structures of all investigated isomers are given in Fig. 4.

### Structural alterations

For three chosen isomers, the most stable (isomer 5), the shallowest (isomer 12) and the deepest (isomer 16), Fig. 5, bond length alterations are shortly discussed. Bonds are denoted in Fig. 6. In the vicinity of boron atoms some significant bond length alterations happened. Results concerning stability factors and bowl depth for isomers 5, 12 and 16 are summarized in Fig. 7.

For isomer 5, the only significant change in bond length happened for bonds denoted as  $r_{20}$  and  $r_8$ . In this case, the bond length decreased for 3 %. For isomer 12 the most significant bond length alterations happened in the ring in which two carbon atoms were substituted with boron atoms. The bond between two boron atoms, denoted as  $r_{23}$ , increased for 25 %, bond lengths denoted as  $r_{22}$  and  $r_{24}$  increased for 10 % while bond lengths denoted as  $r_1$  increased for 6 %. For isomer 16, the rim containing substituted boron atoms suffered mostly from bond alterations. In this case, the mean value of rim bond length increased for 6 %. The bond length between two boron atoms, denoted as  $r_4$ , increased for 11 %.

Concerning the mean bond length of investigated structures the highest increase happened for isomers 12 and 16 where the mean bond length increased for approximately 4 % comparing with regular sumanene, while for isomer 5 the mean bond length increased for approximately 2 %.

### NICS and chemical shielding

In this chapter we present results concerning chemical shielding and NICS of the further investigated structures. The results of disubstituted sumanenes are compared with chemical shielding and NICS of the regular sumanene. In this way we can deduce where significant changes of the charge density in the investigated structure happened.

We also dealt with zz component of NICS since there are papers stating that this is sometimes better to use for estimation of the aromaticity. Namely, based on the work of [27, 28] the component corresponding to the principal axis perpendicular to the ring plane, NICS<sub>zz</sub>, is found to be a good measure for the characterization of the  $\pi$  system of the ring, because isotropic NICS values at ring centers contain large influences from the  $\sigma$

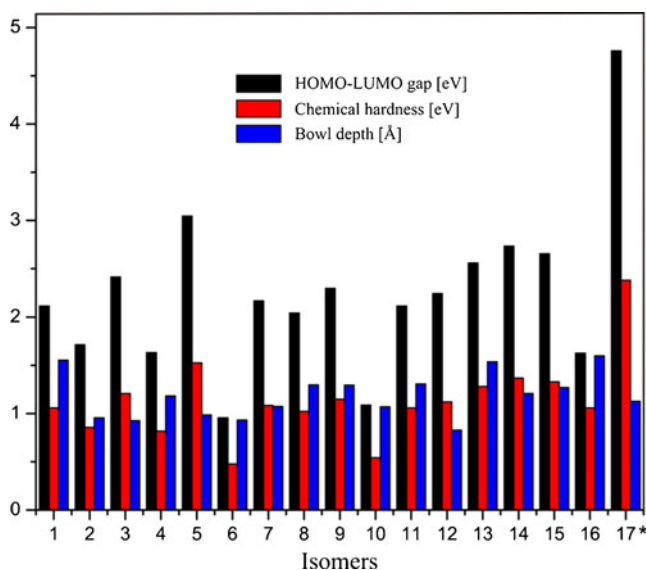
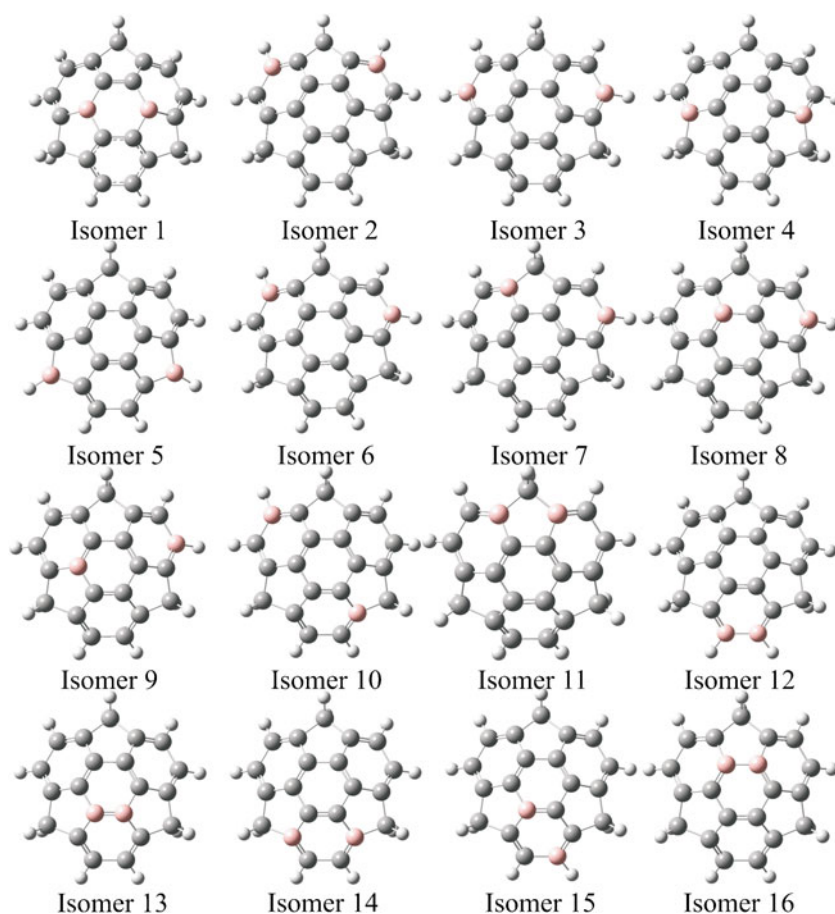


Fig. 3 Stability factors and bowl depth, \*regular sumanene

**Fig. 4** Investigated isomers

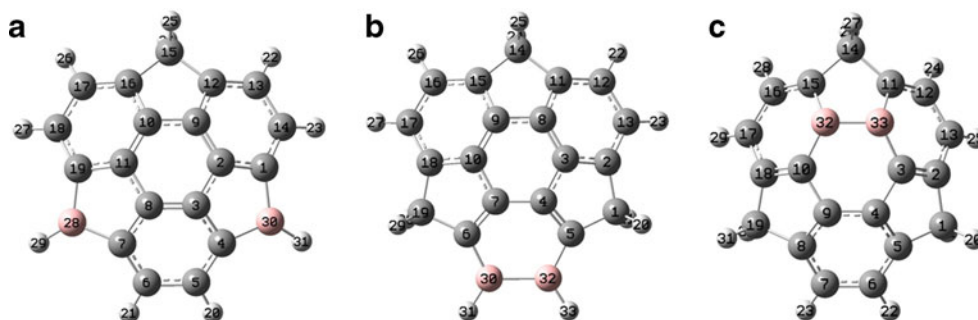
system and from all three principal components of the NICS tensor. At large distances from the ring center, *zz*-component of NICS, which is dominated by contributions from the  $\pi$  system, characterizes NICS better than isotropic value.

In Figs. 8, 9, and 10 we present calculated chemical shielding, NICS and NICS<sub>zz</sub> of isomers compared with chemical shielding, NICS and NICS<sub>zz</sub> of regular sumanene.

Concerning NICS and NICS<sub>zz</sub> of the most stable isomer, the significant changes occurred for the NICS 3, 4 and 5. Aromatic nature of NICS 4 was reversed by introduction of boron atoms from medium aromatic to non-aromatic according to both NICS and NICS<sub>zz</sub>. The NICS 0 value, which corresponds to hub benzene ring, and which might be important for  $\pi$ -stacking, tends to be increased in the aromatic

direction by introduction of boron atoms, while corresponding NICS<sub>zz</sub> value tends to reverse aromatic nature from non-aromatic to aromatic. On the other hand introduction of boron atoms did not affect the chemical shielding parameters much, bearing in mind their sensitivity to the structural alterations.

The substitution of two nitrogen atoms with two boron atoms led to significant changes in the NICS values of isomer 12, Fig. 9. The aromatic property of hub benzene ring, NICS 0, reversed from  $-3.12$  to  $7.67$  according to NICS parameter, but according to NICS<sub>zz</sub> parameter the aromatic property of hub ring increased its non-aromatic nature extremely, from  $14.41$  to  $43.13$  ppm. The aromatic nature of NICS 2 and NICS 6 was reduced according to NICS value, but was reversed according to NICS<sub>zz</sub>. The aromatic nature of NICS 4 was extremely

**Fig. 5** Investigated isomers: **a** 5, **b** 12 and **c** 16.

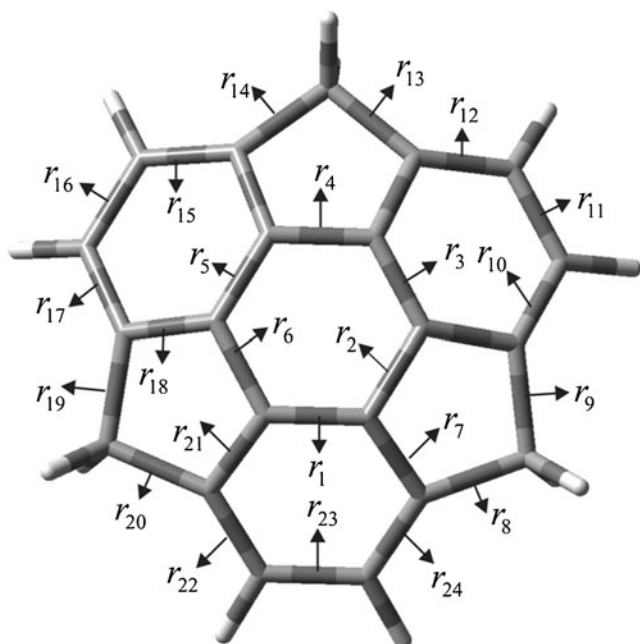
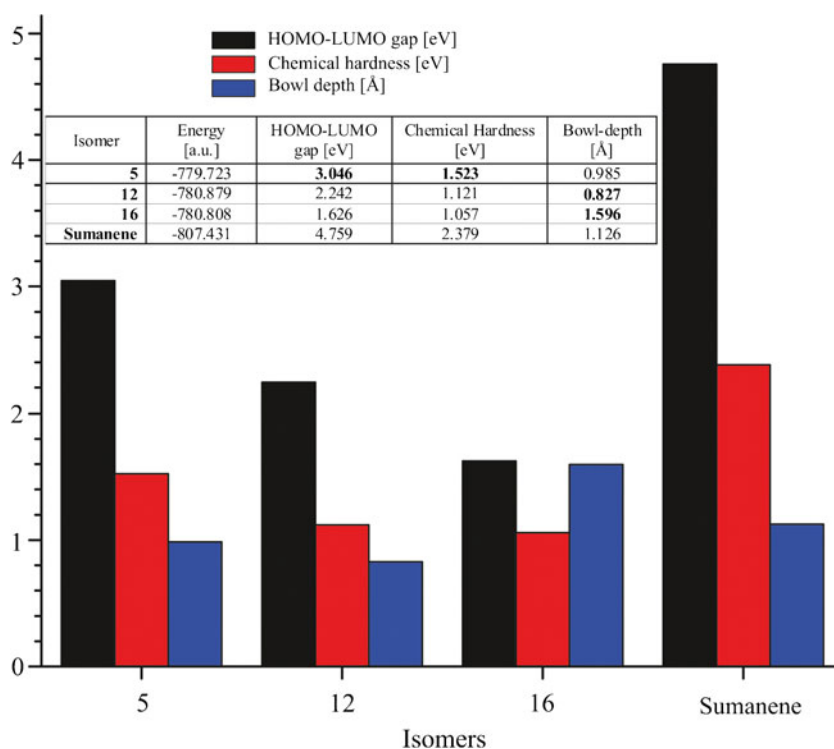


**Fig. 6** Bond denotation

reversed according to both NICS and NICS<sub>zz</sub> parameters, which was expected since this ring contains boron atoms. By introduction of boron atoms only two hub carbon atoms which at the same time belong to the ring that contain boron atoms, suffered from the significant change of chemical shielding.

For isomer 16 the introduction of two boron atoms instead of carbon atoms led to the significant changes of both

**Fig. 7** Stability factors of further investigated isomers and sumanene



NMR parameters, Fig. 10. The aromatic natures of NICS 2 and NICS 6 reversed highly according to both parameters, while the highest change happened for hub ring, containing boron atoms. Also, for this isomer the introduction of boron atoms led to the most significant changes of chemical shielding among all further investigated isomers.

#### Bowl to bowl inversion barrier

Bowl to bowl inversion is a characteristic feature of some flexible  $\pi$ -bowls [1]. This property has been intensively studied with structures based on corannulene, while one of the first results came from Scot et al. [28]. Significant results concerning bowl to bowl inversion barrier including corannulene came from Wu and Siegel [29].

Employing the same level of theory as for the geometry optimizations and NMR parameters for the bowl-to-bowl inversion barrier we obtained the value of 16.8 kcal mol<sup>-1</sup> for regular sumanene. Amaya et al. [30] reported for the inversion barrier of regular sumanene the value of 16.9 kcal mol<sup>-1</sup> employing B3LYP/cc-pVTZ//B3LYP/cc-pVDZ level of theory. On the other side, the experimental bowl-to-bowl inversion barrier for sumanene is stated to be ca. 20 kcal mol<sup>-1</sup> (ranging from 19.6 to 20.4 depending on used solvents) [30]. In several other papers, such as [31], the use of semi-empirical methods (MNDO) led to the overestimation, ca. 24 kcal mol<sup>-1</sup> which is to be expected.

For calculations of the bowl-to-bowl inversion barriers we employed the same strategy as in reference [31]. The bowl-to-

**Fig. 8** Comparison of NMR parameters of isomer 5, the most stable one, with regular sumenene: **a** NICS parameters, **b** Chemical shielding, NICS<sub>zz</sub> values are *underlined*

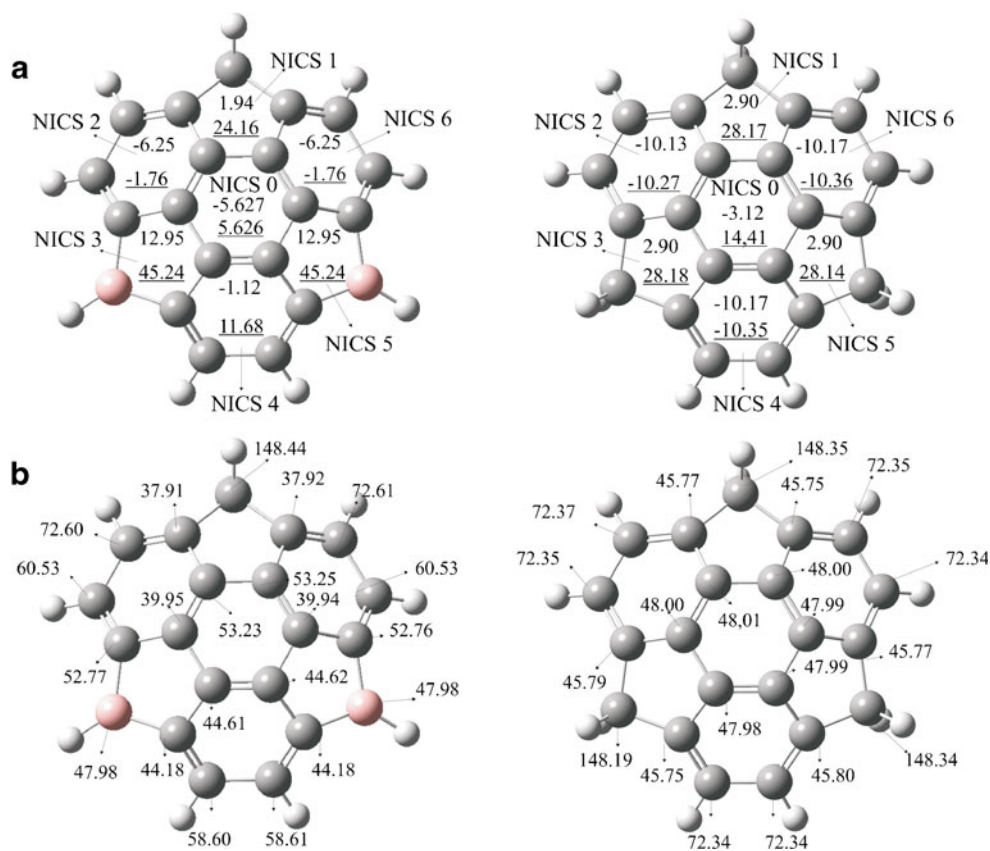


**Fig. 9** Comparison of NMR parameters of isomer 12 with regular sumanene: **a** NICS parameters, **b** Chemical shielding, NICS<sub>zz</sub> values are *underlined*

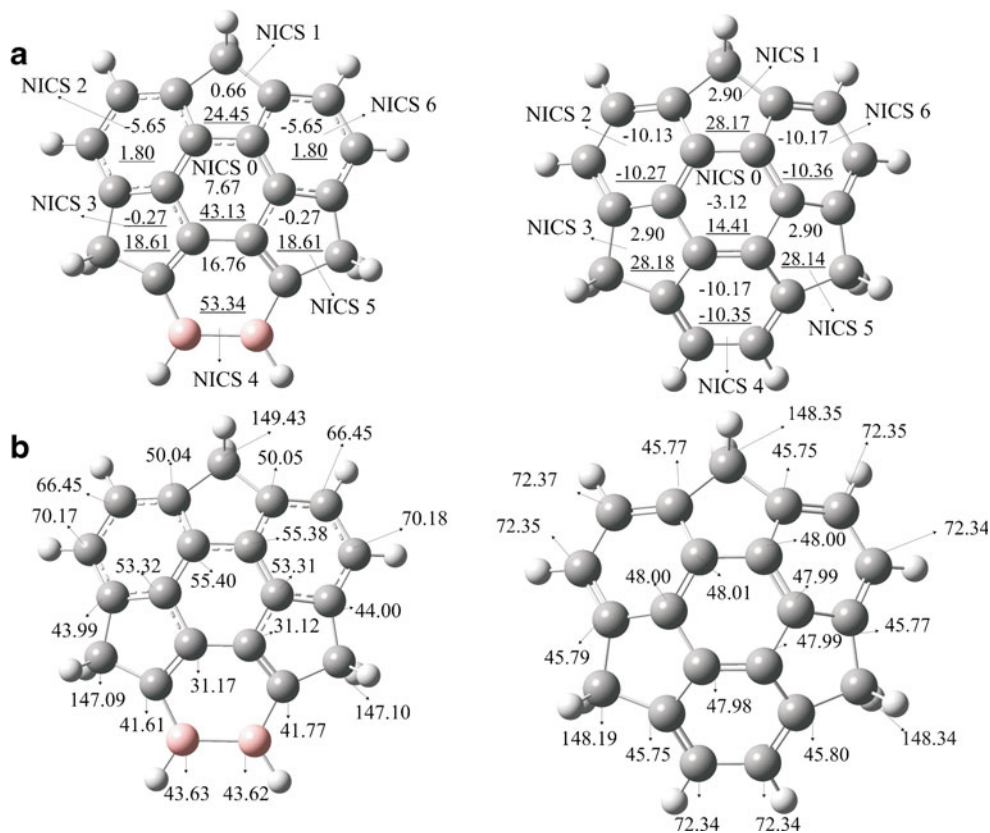
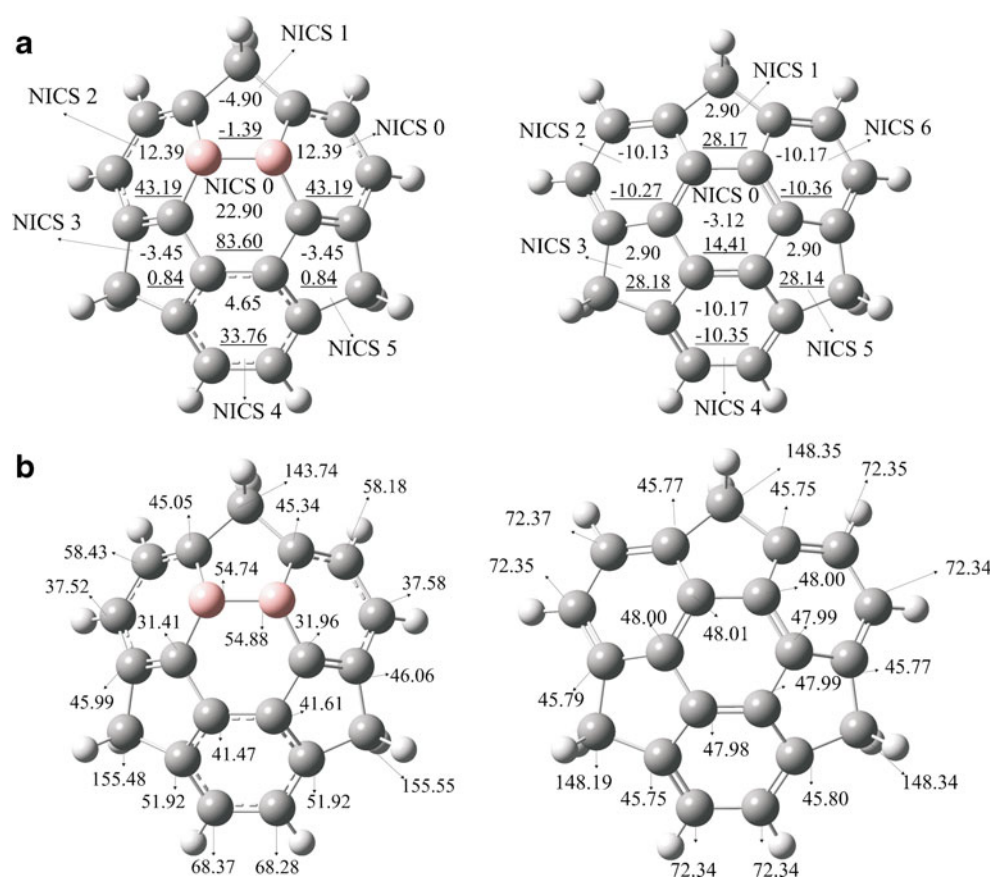


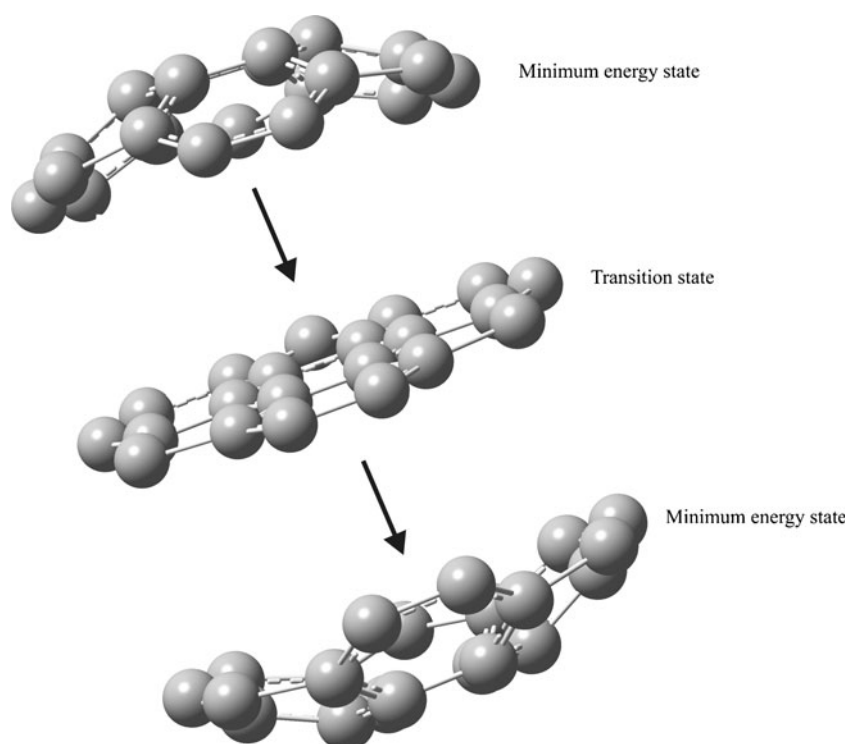
**Fig. 10** Comparison of NMR parameters of isomer 16 with regular sumanene: **a** NICS parameters, **b** Chemical shielding. NICS<sub>zz</sub> values are *underlined*



bowl inversion barriers were calculated from the energy difference between the optimized bowl structure and the planar structure for a transition state. For the time being we did not

investigate solvent effects for the energy barrier calculations, we plan to perform that in following works. Process of bowl to bowl inversion is illustrated on Fig. 11.

**Fig. 11** Illustration of bowl to bowl inversion process



For isomer 5, the most stable one, we had an easy situation. The frequency check result of the minimum energy structure showed no imaginary frequencies indicating that we are dealing with the structure with the true minimum. Further we employed the synchronous transit-guided Quasi-Newton method [32, 33] as implemented in Gaussian 03 in order to locate transition state. We defined guess structure as the planar one and after optimization to the transition state we conducted frequency check which confirmed the existence of one and only one imaginary frequency whose visualization confirmed that it corresponds to the inversion of the observed isomer.

The situation was a little more complicated for isomers 12 and 16. We looked for transition states in the same manner as we did for isomer 5, and after frequency check of obtained transition state for both isomers we received two imaginary frequencies. In both cases, the normal mode corresponding to the one imaginary frequency had a direction corresponding to a bowl-to-bowl inversion, while the consequence of the other imaginary frequency was the torsion of the part of molecule containing boron atoms, along the direction of the corresponded normal mode. We further slightly shifted the obtained structure along the normal mode which corresponded to the imaginary frequency we wanted to eliminate then optimized it to a minimum and carried out the frequency check. Frequency check contained one negative frequency. Then we used this structure as an initial guess structure for transition state for transit-guided Quasi-Newton method and after optimization to the transition state we checked it by frequency analysis. With this approach we were able to locate the transition state for the isomer 12, for which it can be concluded that its transition state is not completely a planar structure, but it is very close. On the other hand, the transition state of isomer 16 is far from planar structure and therefore it can not be used for estimation of the bowl-to-bowl inversion barrier.

The results we obtained for bowl-to-bowl inversion barriers of isomers 5 and 12 are given in Table 1.

For isomer 5, the most stable one the bowl-to-bowl inversion barrier has almost twice lower value for regular sumanene, indicating that this one is more likely to be subjected to the inversion than regular sumanene. For isomer 12, the bowl to bowl barrier is the lowest what is not surprising at all because this isomer is the shallowest.

**Table 1** Bowl to bowl inversion barrier for isomers 5, 12 and sumanene

Isomer	Inversion barrier [kcal mol <sup>-1</sup> ]	Bowl depth [Å]	Chemical hardness [eV]
5	9.087	0.985	1.523
12	4.178	0.827	1.121
Sumanene	16.800	1.126	2.379

## NICS vs. bowl depth

Bearing in mind that the NICS values are closely related to the energetic, structural and magnetic properties of molecules, and that one of the specific quantities of molecular bowls is

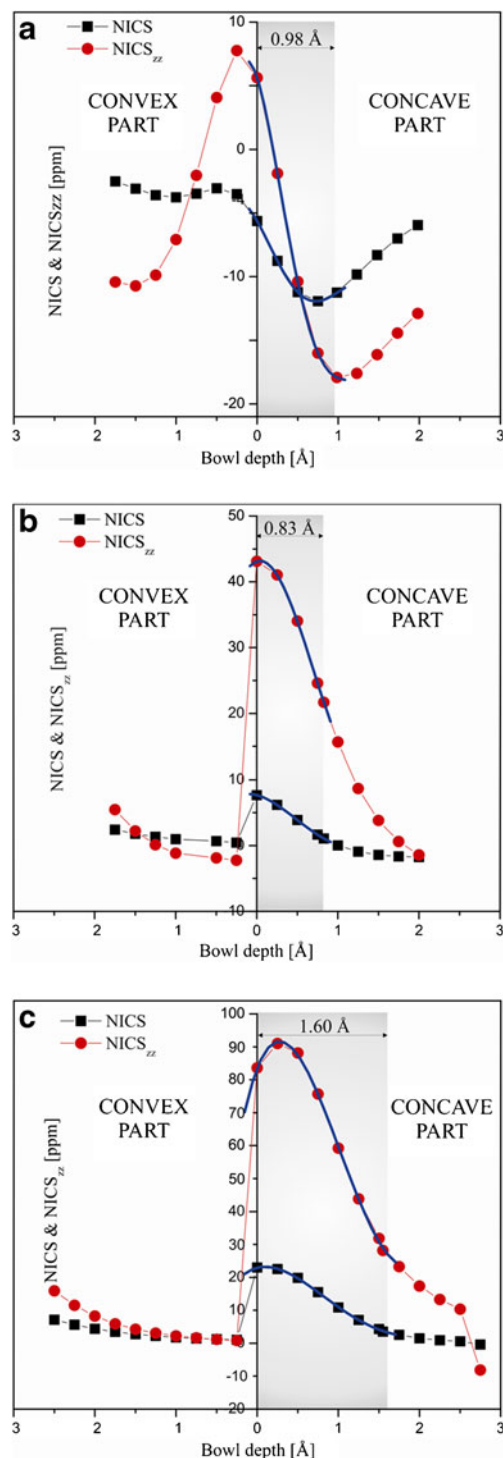


**Fig. 12** Dependence of NICS on bowl depth for isomers: **a** 5, **b** 12 and **c** 16



bowl depth, it is useful to make an effort to correlate these two quantities.

In their theoretical treatment for metallacyclopentene ring inversion, Burgi and Dubler-Steudle [34] have shown that there exists attractive and repulsive parts which results in a double well potential. The same approach Priyakumar and Sastry [35] used in their work. In that approach Burgi has observed the change in energy along the reaction path for automerization and described it by the double-well potential, given as follows:

$$E = ax^4 - bx^2 \tag{3}$$

where  $x$  is bowl depth.

For the equilibrium geometry of the bowl structure, or in other words at the minimum of investigated structure the first derivative of energy along the reaction coordinate vanishes so further we have:

$$4ax^3 - 2bx = 0 \tag{4}$$

Solving the last equation we receive:

$$x^2 = \frac{b}{2a} \rightarrow b = 2ax_{eq}^2 \tag{5}$$

**Table 2** NPA charges of isomers 5, 12, 16 and sumanene

Atom number	Sumanene	Isomer 5	Isomer 12	Isomer 16
1.	-0.410	(B) 0.615	-0.478	-0.483
2.	0.104	-0.377	0.019	-0.026
3.	<b>0.012</b>	<b>0.017</b>	<b>-0.045</b>	<b>-0.220</b>
4.	<b>0.012</b>	<b>-0.007</b>	<b>0.028</b>	<b>-0.023</b>
5.	0.103	-0.333	-0.342	0.011
6.	-0.206	-0.179	(B) <sup>a</sup> 0.320	-0.226
7.	-0.206	-0.179	(B) <sup>a</sup> 0.320	-0.227
8.	0.103	-0.333	-0.341	0.012
9.	<b>0.012</b>	<b>-0.007</b>	<b>0.028</b>	<b>-0.024</b>
10.	<b>0.012</b>	<b>-0.036</b>	<b>-0.022</b>	<b>(B)<sup>a</sup> 0.288</b>
11.	<b>0.012</b>	<b>-0.036</b>	<b>-0.022</b>	<b>(B)<sup>a</sup> 0.288</b>
12.	<b>0.012</b>	<b>0.017</b>	<b>-0.045</b>	<b>-0.219</b>
13.	0.103	0.031	-0.004	-0.145
14.	-0.206	-0.248	-0.213	-0.279
15.	-0.206	-0.163	-0.232	-0.123
16.	-0.410	-0.484	-0.476	-0.479
17.	0.104	0.031	-0.004	-0.145
18.	-0.206	-0.248	-0.213	-0.280
19.	-0.206	-0.163	-0.232	-0.123
20.	0.103	-0.377	0.019	-0.027
21.	-0.410	(B) 0.615	-0.478	-0.483

<sup>a</sup> Boron atoms. Hub atoms are given in bold style

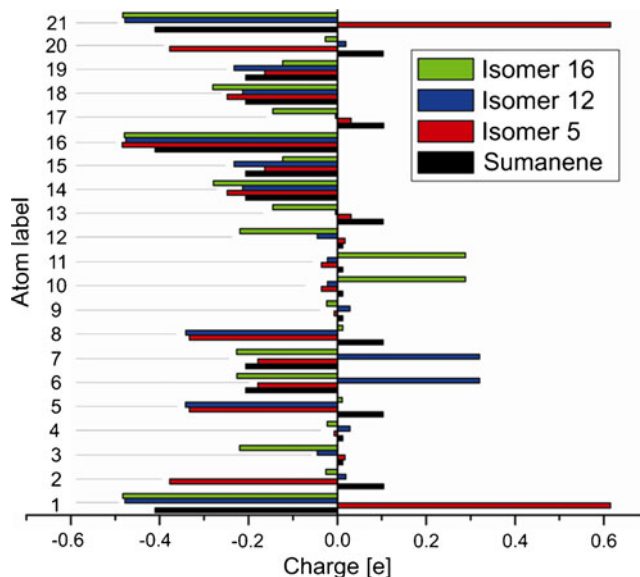


**Fig. 13** Charges of isomers 5, 12, 16 and regular sumanene

Bearing in mind that the barrier height is given by relation:

$$-\Delta E = E(x_{eq}) - E(x_0) \tag{6}$$

where  $E(x_{eq})$  is equilibrium energy of structure (when we have equilibrium bowl depth), while  $E(x_0)$  is energy of transition state, one finally obtains:

$$-\Delta E = (ax_{eq}^4 - 2ax_{eq}^2x_{eq}^2) - 0 = -ax_{eq}^4 \tag{7}$$

where  $x_{eq}$  is bowl depth at the minimum of energy (equilibrium bowl depth), while  $x_0$  is the bowl depth in the transition state. Of course, since the transition state is planar structure, it is clear that  $x_0=0$ .

In other words, the conclusion is that quartic function finely correlates the bowl-to-bowls inversion barrier with bowl depth.

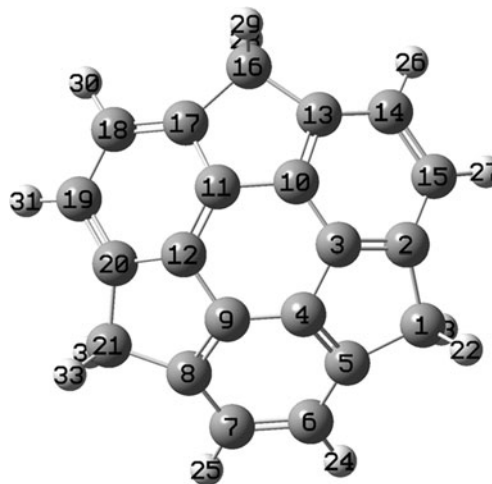


**Fig. 14** Numbering scheme for NPA analysis

**Table 3** Significant interactions in NBO analysis of isomer 5

Interaction	Donor NBO (i)	Acceptor NBO (j)	E(2) kcal mol <sup>-1</sup>
1.	BD (2) C1–C14	LP*(1) B30	20.77
2.	BD (2) C4–C5	LP*(1) B30	18.34
3.	BD (2) C6–C7	LP*(1) B28	18.34
4.	BD (2) C18–C19	LP*(1) B28	20.77
5.	LP*(1) B28	BD*(2) C6–C7	31.65
6.	LP*(1) B28	BD*(2) C18–C19	38.11
7.	LP*(1) B30	BD*(2) C1–C14	38.10
8.	LP*(1) B30	BD*(2) C4–C5	31.64
9.	BD*(2) C1–C14	BD*(2) C2–C9	151.01
10.	BD*(2) C4–C5	BD*(2) C3–C8	112.53
11.	BD*(2) C6–C7	BD*(2) C3–C8	112.42
12.	BD*(2) C12–C13	BD*(2) C2–C9	135.98
13.	BD*(2) C16–C17	BD*(2) C10–C11	135.94
14.	BD*(2) C18–C19	BD*(2) C10–C11	151.06

Bearing in mind that the double-well potential is simply a function of  $x$  (where  $x$  is the bowl-depth) it means that the quartic function of  $x$  fits the activation energy change of the ring-inversion. This was the result valid for series of metal-cyclopentenes in the study of Burgi and Dubler-Steudle [34].

In our work we concluded that the quartic function of bowl depth not only finely correlates the bowl-to-bowl inversion barrier with bowl depth, but also finely correlates change of NICS and NICS<sub>zz</sub> with bowl depth. The results are given in Fig. 12.

In Fig. 12 we present the change of NICS and NICS<sub>zz</sub> values with bowl depth. Left side of graph corresponds to the convex part while right side corresponds to the concave part of sumanene isomer. For this purpose we placed a set of ghost atoms on the line that connects the ghost atom in the centroid of hub atoms and ghost atom in the centroid of rim atoms in both concave and convex part of the bowl like isomer. Ghost atoms were placed in steps of 0.25 Å.

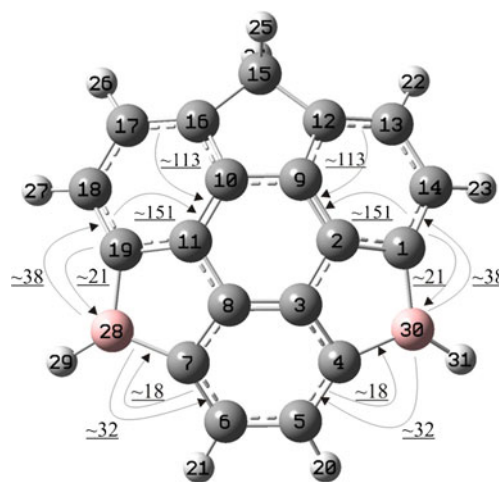
As can be seen from Fig. 12 for all isomer changes of the NICS values are consistent with the changes of the NICS<sub>zz</sub>. An important conclusion is that the values of both NICS and NICS<sub>zz</sub> increase quartically with the increase of bowl depth.

Here arises the logical question; which NICS value to use for description of the aromaticity; isotropic value or zz component. This topic is popular and there are several papers published in the valuable journals that are dealing exclusively with parameters that can be used for the aromaticity estimation. We dealt with this question in our previous paper [36] where we investigated the aromaticity of the active components of frequently used  $\beta$ -blockers. It turned out there that changes of the NICS values were not consistent with changes of chemical hardness, in contrast to the NICS<sub>zz</sub> values which changes were consistent with changes of chemical hardness. As we dealt in that work with

structures for which aromatic ring is dimensionally comparable with the rest of the molecule we practically stated that the aromaticity is related with stability (H-L gap, chemical hardness). Such conclusion cannot be drawn here as we are dealing with structures with more than one aromatic ring beside the fact that one aromatic ring of sumanene is much smaller than the whole molecule.

What we can perform in this situation is that we can observe in more detail the changes of NICS values with bowl depth in the way we described in the beginning of this subchapter.

It can be seen from Fig. 12 that changes of the NICS<sub>zz</sub> values are more intensive than changes of the NICS values and that changes are mutually consistent. Therefore any type of correlation between the NICS/NICS<sub>zz</sub> values and some other parameter can be more visible if one observes the NICS<sub>zz</sub>.

**Fig. 15** Significant interactions (kcal mol<sup>-1</sup>) in NBO analysis of isomer 5

**Table 4** Significant interactions (in kcal mol<sup>-1</sup>) in NBO analysis of isomer 12

Interaction	Donor NBO (i)	Acceptor NBO (j)	E(2) kcal mol <sup>-1</sup>
1.	BD (2) C4–C5	LP*(1) B32	26.03
2.	BD (2) C6–C7	LP*(1) B30	26.00
3.	LP*(1) B30	BD*(2) C6–C7	24.74
4.	LP*(1) B32	BD*(2) C4–C5	24.79
5.	BD*(2) C12–C13	BD*(2) C2–C3	147.24
6.	BD*(2) C12–C13	BD*(2) C8–C11	139.36
7.	BD*(2) C16–C17	BD*(2) C9–C15	139.23
8.	BD*(2) C16–C17	BD*(2) C10–C18	147.32

Bearing in mind what we said concerning the NICS<sub>zz</sub>, based on [28] it can be concluded that when the NICS and NICS<sub>zz</sub> take the same or similar values there is no large influence of  $\sigma$  system and all three principal components of the NICS tensor and that these two parameters are equivalent to evaluate aromaticity. If we draw changes of the NICS/NICS<sub>zz</sub> values with bowl depth, mentioned values we can obtain as the intersections of lines that represent changes of the NICS/NICS<sub>zz</sub> values with bowl. For isomer 5 the picture is symmetric not only from the aspect of intersection but also from the aspect of slope which is similar from both sides.

For isomer 12, on graph b, contrary to isomer 5 slopes of both sides are very different. Slope in the convex part is much higher than the slope in the concave part due to the geometry of structure. There are practically two intersections on the convex part, and the change between NICS and NICS<sub>zz</sub> values is small, indicating that influences of  $\sigma$  system and three principal components of NICS tensor are low.

In the graph c picture is not symmetric. This is not strange since that isomer is the deepest of all investigated and therefore the influences of geometry on the NICS are much higher in the concave part and the difference between the NICS and NICS<sub>zz</sub> is the highest of all investigated isomers. Again, due to the geometry, slope of NICS dependence on bowl depth, in convex part is the largest.

#### NBO and NPA analysis

An efficient method for studying intra and inter molecular bonding and interaction among bonds is represented by natural bond order (NBO) analysis. It provides an efficient method for studying intra and inter molecular bonding and interaction among bonds; it is a convenient basis for investigation of charge transfer or conjugative interactions in molecular system [37–41].

NBO analysis is carried out by energetic examination of all possible interactions between ‘filled’ (donor) NBOs and ‘empty’ (acceptor) NBOs, and estimating their energetic importance by 2nd-order perturbation theory. In this manner we obtained the energies of delocalization of electrons from

filled NBOs into empty NBOs, e.g., we obtain stabilization energies gained by donation from the donor NBO to the acceptor NBO. In this way we are able to conclude which interactions among all possible interactions produce stability for certain molecule.

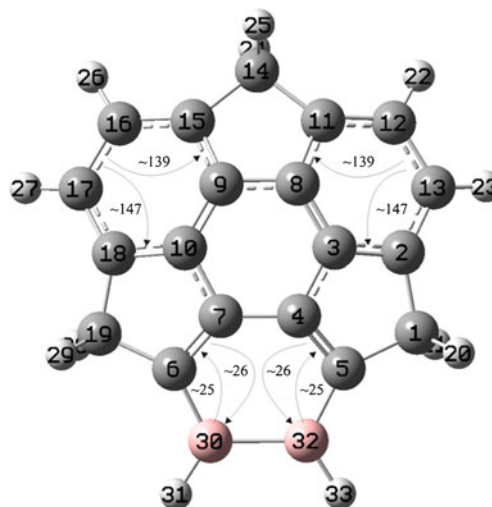
For each donor NBO (i) and acceptor NBO (j), the stabilization energy associated with  $i \rightarrow j$  delocalization can be estimated on the basis of second order perturbation theory as:

$$E(2) = \Delta E_{ij} = q_i \frac{F(i,j)^2}{\varepsilon_i \varepsilon_j} \quad (8)$$

where  $q_i$  is the donor orbital occupancy,  $\varepsilon_i$ ,  $\varepsilon_j$  are diagonal elements (orbital energies) and  $F(i,j)$  is the off-diagonal NBO Fock matrix element.

In Tables 3, 4, and 5, the perturbation energies of significant donor–acceptor interactions are summarized and three highest values are indicated on diagrams. The larger the  $E(2)$  value, the intensive is the interaction between electron donors and electron acceptors.

To study the charge distribution of some molecules it is better to use natural population analysis (NPA) than Milliken one, since NPA do not exhibit dependence on basis set [42].

**Fig. 16** Significant interactions (in kcal mol<sup>-1</sup>) in NBO analysis of isomer 12

**Table 5** Significant interactions in NBO analysis of isomer 16

Interaction	Donor NBO (i)	Acceptor NBO (j)	E(2) kcal mol <sup>-1</sup>
1.	BD (2) C2–C3	LP*(1) B33	20.49
2.	BD (2) C10–C18	LP (1) C17	61.75
3.	BD (2) C10–C18	LP*(1) B32	20.45
4.	BD (2) C12–C13	LP*(1) C11	58.58
5.	BD (2) C15–C16	LP (1) C1	73.66
6.	BD (2) C15–C16	LP*(1) B32	15.85
7.	LP*(1) C11	LP*(1) B33	67.68
8.	LP*(1) C11	BD*(2) C12–C13	57.70
9.	LP (1) C17	BD*(2) C10–C18	38.82
10.	LP (1) C17	BD*(2) C15–C16	40.84
11.	BD*(2) C12–C13	BD*(2) C2–C3	73.04

Buckybowls are polar in contrast to the planar aromatic hydrocarbons because of the anisotropic distribution of  $\pi$ -electrons and the C–H bonds, which is the trigger for separation of charges [43]. This is confirmed by results in Table 2 where charges of atoms are given for sumanene and investigated isomers.

It can be seen that the hub atoms have positive charge while the rim atoms have negative charge. The introduction of the boron atoms instead of the carbon atoms changed significantly the charge of other atom. The atom charges are visually summarized in Fig. 13 for which numbering scheme given in Fig. 14 is used.

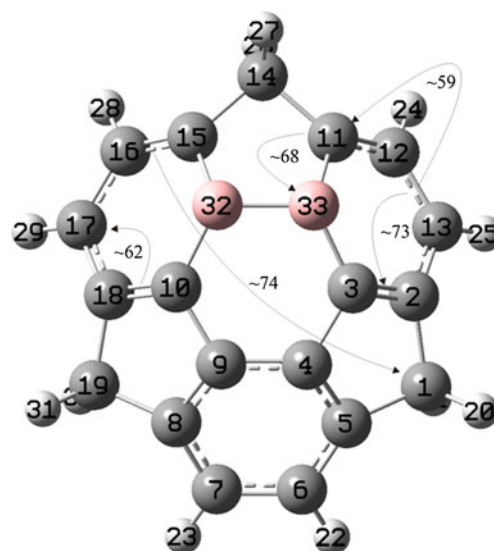
High positive values on the right side of histogram correspond to boron atoms.

If we look in Table 3 and Fig. 15, we can see that lone pairs located on the boron atoms, denoted as LP\*(1) B28 and LP\*(1) B30 are donors to the orbitals located between the closest carbon atoms from both sides. More precisely, LP\*(1) B28 has important donor activity to the bonds between C6–C7 and C18–C19. Symmetrically to that, the lone pair on the opposite boron atom, denoted as LP\*(1) B30 has expressed donor activity to the bonds between C4–C5 and C1–C14. The interaction energies for these cases are around 31 and 38 kcal mol<sup>-1</sup>. Further, for isomer 5, there exist strong donor-acceptor interactions between BD\*(2) C18–C19 and BD\*(2) C10–C11 and between BD\*(2) C16–C17 and BD\*(2) C10–C11. The consequence of this is that some hub carbon atoms of isomer 5 have negative charge.

Concerning isomer 12, donor/acceptor activity of the lone pairs located on the boron atoms is almost equal, Table 4, therefore hub atoms, denoted as C7 and C4 in Fig. 16, remain positively charged, but higher than in the regular sumanene. This is not the situation with opposite two hub atoms, C8 and C9 and atoms C10 and C3 which are highly influenced by donor activities of BD\*(2) C12–C13 and BD\*(2) C16–C17 to BD\*(2) C2–C3, BD\*(2) C8–C11, BD\*(2) C9–C15 and BD\*(2) C10–C18 because of these mentioned atoms are negatively charged.

Concerning isomer 16, Table 5 and Fig. 17, for its overall stability in general, the lone pairs located on C1, C11, C17 and B33 play an important role. The most significant interaction including the lone pair is between BD(2) C15–C16 and LP (1) C1 which is possible due to the high bowl depth, because of which the mentioned atoms are significantly closer than in the regular sumanene. On the other hand the most significant interaction is between BD\*(2) C12–C13 and BD\*(2) C2–C3. Further, the interaction between two lone pairs, LP\* (1) C11 and LP\*(1) B33 is also significant.

In general, for isomer 5 there are six interactions, for isomer 12 there are four interactions while for isomer 16 there are no interactions with values more than 100 kcal mol<sup>-1</sup>. Further, as can be seen from Tables 3, 4, and 5 number of significant interactions between electron donors and electron acceptors is the largest for isomer 5 than comes isomer 12 and 16 indicating again that isomer 5 is the most stable since there are more interactions that contribute to the stability of molecule.

**Fig. 17** Significant interactions (in kcal mol<sup>-1</sup>) in NBO analysis of isomer 16

This decrease in number of stronger interactions is consistent with the decrease of chemical hardness, from isomer 5 to isomer 16.

## Conclusions

In this paper we investigate sumanene isomers obtained by substitution of two carbon atoms with two boron atoms. Among 16 isomers which were subjected to the bowl-depth and stability analysis, we subjected three isomers to further investigation that included calculations of the NMR parameters, NICS and the bowl-to-bowl inversion barriers.

According to mentioned stability factors the most stable isomer was isomer 5 with HOMO-LUMO gap of 3.046 eV and chemical hardness of 1.243 eV, although these values were also significantly high for isomers 12 and 16.

The mean bond value compared to the regular sumanene increased for all three isomers while the most pronounced increase happened for isomer 16.

When considering the NMR parameters introduction of boron atoms caused significant changes in the NICS, NICS<sub>zz</sub> and chemical shielding values. The highest change happened for the NICS 0 value, according to both NICS and NICS<sub>zz</sub>. Also, changes of chemical shielding were very significant for this isomer especially for the carbon atoms located on the rings containing substituted boron atoms.

We managed to locate transition states of further investigated isomers. Transition state was the easiest to find for the most stable isomer— isomer 5. For this isomer we gained the planar transition state structure with only one imaginary frequency straightforwardly. For isomer 12 we obtained the planar transition state but with two imaginary frequencies and therefore we had to displace obtained structure along the direction of the normal mode corresponding to the spurious frequency and optimized it to the minimum with frequency check. In this manner we successfully obtained the transition state which was not fully planar, but was characterized with only one imaginary frequency indicating that it was the true transition state.

For isomer 16 a true transition state was far away from planar form so it could not be used for estimation of the bowl-to-bowl inversion barrier.

We also correlated the change of the NICS parameters with bowl depth. The conclusion is that quartic function of bowl depth not only finely correlate the bowl-to-bowl inversion barrier with bowl depth, but also finely correlate change of the NICS and NICS<sub>zz</sub> with the bowl depth.

The NBO/NPA analysis gave further insight into the most significant interactions between electron donors and acceptors which further gave an insight into the charge transfer. In all cases the introduction of the boron atoms violated polarity of the initial regular sumanene.

**Acknowledgments** We express our gratitude to Professor Enrique Louis Cereceda, Departamento de Física Aplicada, Universidad de Alicante and Professor Emilio San Fabián Maroto, Departamento de Química Física, Universidad de Alicante, for help and access to Gaussian 03. Without their support we would not be able to conduct research.

We also express our gratitude to our dear friend and colleague Igor Vragović, Departamento de Física Aplicada, Universidad de Alicante for kind support and very useful guides.

This work is done within the project of the Ministry of Education and Science of Republic of Serbia grant no. OI 171039.

## References

- Amaya T, Hirao T (2011) A molecular bowl sumanene. *Chem Commun* 47:10524–10535
- Sakurai H, Daiko T, Hirao T (2003) A synthesis of sumanene, a fullerene fragment. *Science* 301:1878–1878
- Bianco A (2004) Carbon nanotubes for the delivery of therapeutic molecules. *Expert Opin Drug Deliv* 1:57–65
- Lee H-J, Choi WS, Nguyen T, Lee YB, Lee H (2011) An easy method for direct metal coordination reaction on unoxidized single-walled carbon nanotubes. *Carbon* 49:5150–5157
- Yeung CS, Wang YA (2011) Lewis acidity of Pt-doped bucky-bowls, fullerenes, and single-walled carbon nanotubes. *J Phys Chem C* 115:7153–7163
- Vostrowsky O, Hirsch A (2006) Heterofullerenes. *Chem Rev* 106:5191–5207
- Denis PA (2008) Theoretical investigation of nitrogen disubstituted corannulenes. *J Mol Struct (THEOCHEM)* 865:8–13
- Cauët E, Jacquemin D (2012) A theoretical spectroscopy investigation of oxosumanenes. *Chem Phys Lett* 519:49–53
- Sakurai H, Daiko T, Sakane H, Amaya T, Hirao T (2005) Structural elucidation of sumanene and generation of its benzylic anions. *J Am Chem Soc* 127:11580–11581
- Mehta G, Shah SR, Ravikumar K (1993) Towards the design of tricyclopenta[def, jk', pqr]triphenylene ('sumanene'): a 'bowl-shaped' hydrocarbon featuring a structural motif Present in C<sub>60</sub> (buckminsterfullerene). *J Chem Soc Chem Commun* 12:1006–1008
- Silverstein RM, Webster FX (1997) Spectrometric identification of organic compounds. Wiley, New York
- Ghafouri R, Anafcheh M (2012) A computational NICS and <sup>13</sup>C NMR characterization of C<sub>60-n</sub>Si<sub>n</sub> heterofullerenes (n = 1, 2, 6, 12, 20, 24, 30). *J Clust Sci* 23:469–480
- Corminboeuf C, Fowler PW, Heine T (2002) <sup>13</sup>C NMR patterns of C<sub>36</sub>H<sub>2x</sub> fullerene hydrides. *Chem Phys Lett* 361:405–410
- Anafcheh M, Hadipour NL (2011) A computational NICS and <sup>13</sup>C NMR characterization of BN-substituted <sup>60</sup>C fullerenes. *Phys E* 44:400–404
- Schleyer PVR, Maerker C, Dransfeld A, Jiao H, Van Eikema Hommes NJR (1996) Nucleus-independent chemical shifts: a simple and efficient aromaticity probe. *J Am Chem Soc* 118:6317–6318
- Goldfuss B, Von Ragué SP (1997) Aromaticity in group 14 metalloles: structural, energetic, and magnetic criteria. *Organometallics* 16:1543–1552
- Jiao H, Von Ragué SP, Mo Y, McAllister MA, Tidwell TT (1997) Magnetic evidence for the aromaticity and antiaromaticity of charged fluorenyl, indenyl, and cyclopentadienyl systems. *J Am Chem Soc* 119:7075–7083
- Zywietz TK, Jiao H, Schleyer PVR, De Meijere A (1998) Aromaticity and antiaromaticity in oligocyclic annelated five-membered ring systems. *J Org Chem* 63:3417–3422

19. Becke AD (1988) Density-functional exchange-energy approximation with correct asymptotic behavior. *Phys Rev A* 38:3098–3100
20. Lee C, Yang W, Parr RG (1988) Development of the Colic-Salvetti correlation-energy formula into a functional of the electron density. *Phys Rev B* 37:785–789
21. Wolinski K, Hinton JF, Pulay P (1990) Efficient implementation of the gauge-independent atomic orbital method for NMR chemical shift calculations. *J Am Chem Soc* 112:8251–8260
22. Frisch MJ, Trucks GW, Schlegel HB, Scuseria GE, Robb MA, Cheeseman JR, Montgomery JA, Vreven JRT, Kudin KN, Burant JC, Millam JM, Iyengar SS, Tomasi J, Barone V, Mennucci B, Cossi M, Scalmani G, Rega N, Petersson GA, Nakatsuji H, Hada M, Ehara M, Toyota K, Fukuda K, Hasegawa J, Ishida M, Nakajima T, Honda Y, Kitao O, Nakai H, Klene M, Li X, Knox JE, Hratchian HP, Cross JB, Adamo C, Jaramillo J, Gomperts R, Stratmann RE, Yazyev O, Austin AJ, Cammi R, Pomelli C, Ochterski JW, Ayala PY, Morokuma K, Voth GA, Salvador P, Dannenberg JJ, Zakrzewski VG, Dapprich S, Daniels AD, Strain MC, Farkas O, Malick DK, Rabuck AD, Raghavachari K, Foresman JB, Ortiz JV, Cui Q, Baboul AG, Clifford S, Cioslowski J, Stefanov BB, Liu G, Liashenko A, Piskorz P, Komaromi I, Martin RL, Fox DJ, Keith T, Al-Laham MA, Peng CY, Nanayakkara A, Challacombe M, Gill PMW, Johnson B, Chen W, Wong MW, Gonzalez C, Pople JA (2004) Gaussian Inc, Wallingford, CT
23. Pearson RG (1989) Absolute electronegativity and hardness: applications to organic chemistry. *J Org Chem* 54:1423–1430
24. Parr RG, Chattaraj PK (1991) Principle of maximum hardness. *J Am Chem Soc* 113:1854–1855
25. Chandrakumar KRS, Ghanty TK, Ghosh SK (2004) Relationship between ionization potential, polarizability, and softness: a case study of lithium and sodium metal clusters. *J Phys Chem A* 108:6661–6666
26. Chattaraj PK, Lee H, Parr RG (1991) HSAB principle. *J Am Chem Soc* 113:1855–1856
27. Corminboeuf C, Heine T, Seifert G, Von Ragué SP, Weber J (2004) Induced magnetic fields in aromatic [n]-annulenes—interpretation of NICS tensor components. *Phys Chem Chem Phys* 6:273–276
28. Scott LT, Hashemi MM, Bratcher MS (1992) Corannulene bowl-to-bowl inversion is rapid at room temperature. *J Am Chem Soc* 114:1920–1921
29. Wu Y-T, Siegel JS (2006) Aromatic molecular-bowl hydrocarbons, synthetic derivatives, their structures, and physical properties. *Chem Rev* 106:4843–4867
30. Amaya T, Sakane H, Muneishi T, Hirao T (2008) Bowl-to-bowl inversion of sumanene derivatives. *Chem Commun* 6:765–767
31. Amaya T, Sakane H, Nakata T, Hirao T (2010) *Pure Appl Chem* 82:969–978
32. Peng C, Schlegel HB (1993) Combining synchronous transit and quasi-newton methods for finding transition states. *Isr J Chem* 33:449–454
33. Peng C, Ayala PY, Schlegel HB, Frisch MJ (1996) Using redundant coordinates to optimize equilibrium geometries and transition states. *J Comput Chem* 17:49–56
34. Bürgi H-B, Dubler-Stuedle KC (1988) Empirical potential energy surfaces relating structure and activation energy. 1. Metallacyclopentene ring inversion in (s-cis- $\eta^4$ -butadiene)metallocene complexes and related compounds. *J Am Chem Soc* 110:4953–4957
35. Priyakumar UD, Sastry GN (2001) Heterobucky bowls: a theoretical study on the structure, bowl-to-bowl inversion barrier, bond length alternation, structure-inversion barrier relationship, stability, and synthetic feasibility. *J Org Chem* 66:6523–6530
36. Armaković S, Armaković SJ, Štrajčić JP, Štrajčić IJ (2012) Active components of frequently used  $\beta$ -blockers from the aspect of computational study. *J Mol Model* 18:4491–4501
37. Reed AE, Curtiss LA, Weinhold F (1988) Intermolecular interactions from a natural bond orbital, donor-acceptor viewpoint. *Chem Rev* 88:899–926
38. Rossini AJ, Mills RW, Briscoe GA, Norton EL, Geier SJ, Hung I, Zheng S, Autschbach J, Schurko RW (2009) Solid-state chlorine NMR of group IV transition metal organometallic complexes. *J Am Chem Soc* 131:3317–3330
39. Autschbach J, Zheng S (2008) Analyzing Pt chemical shifts calculated from relativistic density functional theory using localized orbitals: the role of Pt 5d lone pairs. *Magn Reson Chem* 46:S45–S55
40. Autschbach J, Zheng S, Schurko R (2010) Analysis of electric field gradient tensors at quadrupolar nuclei in common structural motifs. *Concepts Magn Reson A* 36:84–126
41. Xavier RJ, Gobinath E (2012) FT-IR, FT-Raman, ab initio and DFT studies, HOMO–LUMO and NBO analysis of 3-amino-5-mercapto-1,2,4-triazole. *Spectrochim Acta A* 86:242–251
42. Irikura KK (1998) Computational thermochemistry: Prediction and estimation of molecular thermodynamics (ACS Symposium Series 677). American Chemical Society, Washington
43. Priyakumar UD, Sastry GN (2001) First ab initio and density functional study on the structure, bowl-to-bowl inversion barrier, and vibrational spectra of the elusive  $C_{3v}$ -symmetric buckybowl: sumanene,  $C_{21}H_{12}$ . *J Phys Chem A* 105:4488–4494